NANO LETTERS

Letter

pubs.acs.org/NanoLett

Ultrafast Room-Temperature Single Photon Emission from Quantum Dots Coupled to Plasmonic Nanocavities

Thang B. Hoang,[†,‡] Gleb M. Akselrod,[‡,§] and Maiken H. Mikkelsen*[,†,‡,§]

[†]Department of Physics, [‡]Center for Metamaterials and Integrated Plasmonics, and [§]Department of Electrical and Computer Engineering, Duke University, Durham, North Carolina 27708, United States

Supporting Information

ABSTRACT: Efficient and bright single photon sources at room temperature are critical components for quantum information systems such as quantum key distribution, quantum state teleportation, and quantum computation. However, the intrinsic radiative lifetime of quantum emitters is typically ~10 ns, which severely limits the maximum single photon emission rate and thus entanglement rates. Here, we demonstrate the regime of ultrafast spontaneous emission (~10 ps) from a single quantum emitter coupled to a plasmonic nanocavity at room temperature. The nanocavity integrated with a single colloidal semiconductor quantum dot produces a 540-fold decrease in the emission lifetime and a simultaneous 1900-fold increase in the total emission intensity. At the same time, the nanocavity acts as a highly efficient optical antenna directing the emission into a single lobe normal to the surface. This plasmonic platform is a versatile geometry into which a variety of other quantum emitters, such as crystal color centers, can be integrated for directional, room-temperature single photon emission rates exceeding 80 GHz.

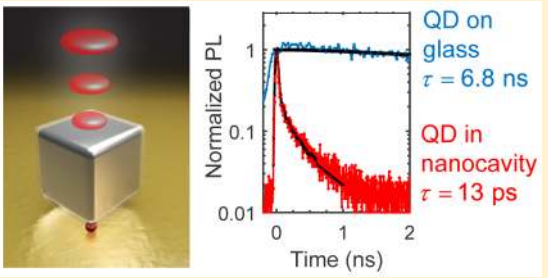

KEYWORDS: *Plasmonics, quantum dots, nanocavity, nanocube, single photon source, quantum optics*

The most common way to generate single photons is to use spontaneous emission from a two-level system, which cannot emit more than one photon simultaneously.[1,2] Typical two-level solid state systems used as single photon sources include molecules,[3] colloidal[4,5] and epitaxial quantum dots (QDs),[6,7] and color centers in crystals such as diamond[8−10] and silicon carbide.[11] A number of factors limit the maximum photon count rate from these emitters including low collection efficiency and low quantum yield. However, the most fundamental limitation on the maximum photon rate is the relatively long intrinsic lifetime (~2−20 ns) of the electronic excited state of typical emitters.

To increase the spontaneous emission rate of the excited state, and hence the maximum single photon rate, the emitter can be placed in a photonic environment with an increased local density of optical states.[12] This increased spontaneous emission rate, known as the Purcell effect, can be achieved by integrating the emitter into an optical cavity with either a small mode volume or a high quality factor (Q). Microcavities with high quality factors have been coupled to nitrogen vacancy centers in diamond[10,13] and epitaxial QDs.[14−16] Yet, despite intensive efforts in the past decade, the maximum enhancements in the spontaneous emission rate (Purcell factors) for single emitters have been limited to $F_p \approx 30$. In addition to the limited enhancements, high-Q cavities require good spectral matching between a narrowband emitter and the narrowband cavity resonance, involving challenging nanofabrication and limiting scalability, and hence high-Q cavities are inherently unsuitable for broadband room temperature emitters.

Alternatively, quantum emitters can be integrated with plasmonic structures, which can offer small optical mode volumes while having a relatively low Q, which avoids the challenge of spectral matching the emitters to the cavity. Single photon emitters coupled to plasmonic structures have been demonstrated using molecules,[17] nitrogen-vacancy centers in nanodiamonds,[8] diamond pillars,[9] epitaxial QDs,[18] and colloidal QDs.[5,19,20] However, as with dielectric cavities, the Purcell factors for single emitters have thus far been limited to ~30 due to relatively large mode volumes. Larger enhancements in the total decay rate have been observed, but the role of radiative rate enhancement is unclear[21] or the nonradiative quenching is dominant.[20] A promising geometry that has been theoretically proposed as a single photon source is the plasmonic patch antenna,[22] which consists of a flat metal nanoparticle situated over a metal ground plane. This structure has been used for large Purcell enhancement of ensembles of molecules,[23] ensembles of QDs,[24,25] and few or single QDs showing multiphoton emission;[26] however, single photon emission has remained an outstanding challenge until now.

Here, we report ultrafast spontaneous emission with a lifetime of ~10 ps from a single QD coupled to a plasmonic structure that acts both as a small mode volume nanocavity and a nanopatch optical antenna. This emission lifetime corresponds to a detector-limited 540-fold enhancement in the

Received: September 15, 2015
Revised: November 20, 2015

DOI: 10.1021/acs.nanolett.5b03724
Nano Lett. XXXX, XXX, XXX−XXX

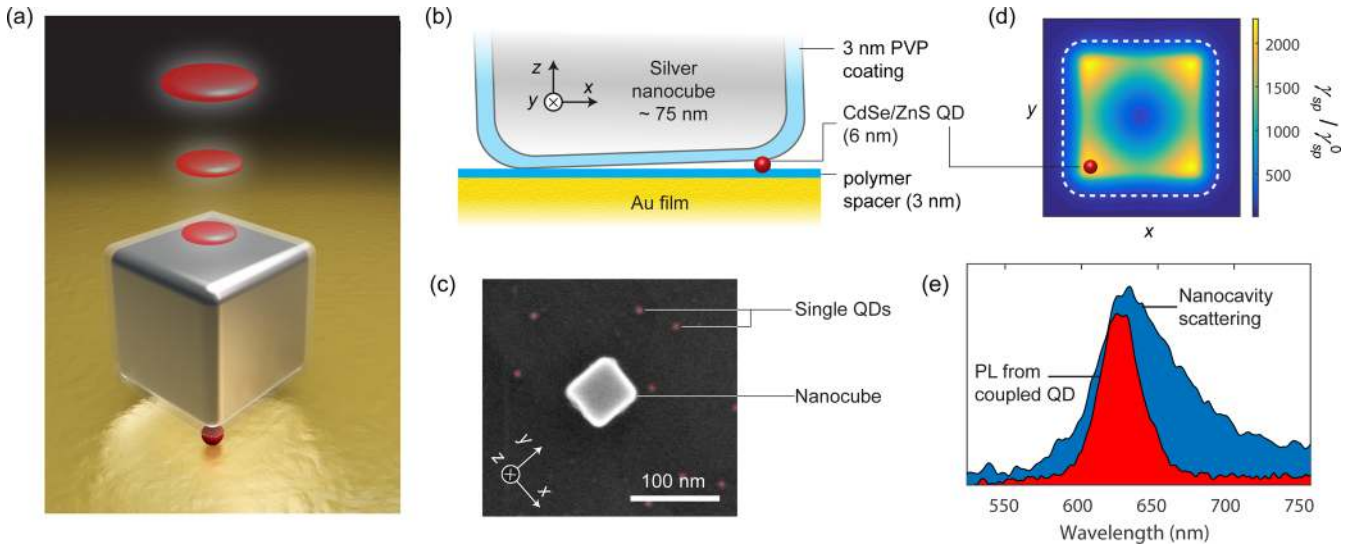

Figure 1. (a) Illustration of a single colloidal QD in the gap between a silver nanocube and a gold film, emitting single photons. (b) Cross-sectional schematic of a single QD embedded in the nanocavity, with the ~6 nm diameter QD located near the corner of the nanocube, where the field enhancements are the largest. (c) SEM image of the sample structure, showing individual QDs and a single nanocube. Some nanocavities contain a single QD in the gap between the nanocube and gold film, which is not visible in SEM images. (d) Simulated enhancement in the spontaneous emission rate γ_{sp} relative to the free space rate γ_{sp}^{0} for a randomly oriented dipole as a function of lateral position in the gap. A single QD is schematically shown near the corner where rate enhancements of ~2000× are expected. (e) Measured scattering spectrum of a single nanocavity (blue) showing a fundamental resonance at λ_{np} = 630 nm. Also shown is photoluminescence (PL) from a single QD coupled to the same antenna (red), with an emission spectrum that overlaps well with the plasmonic resonance.

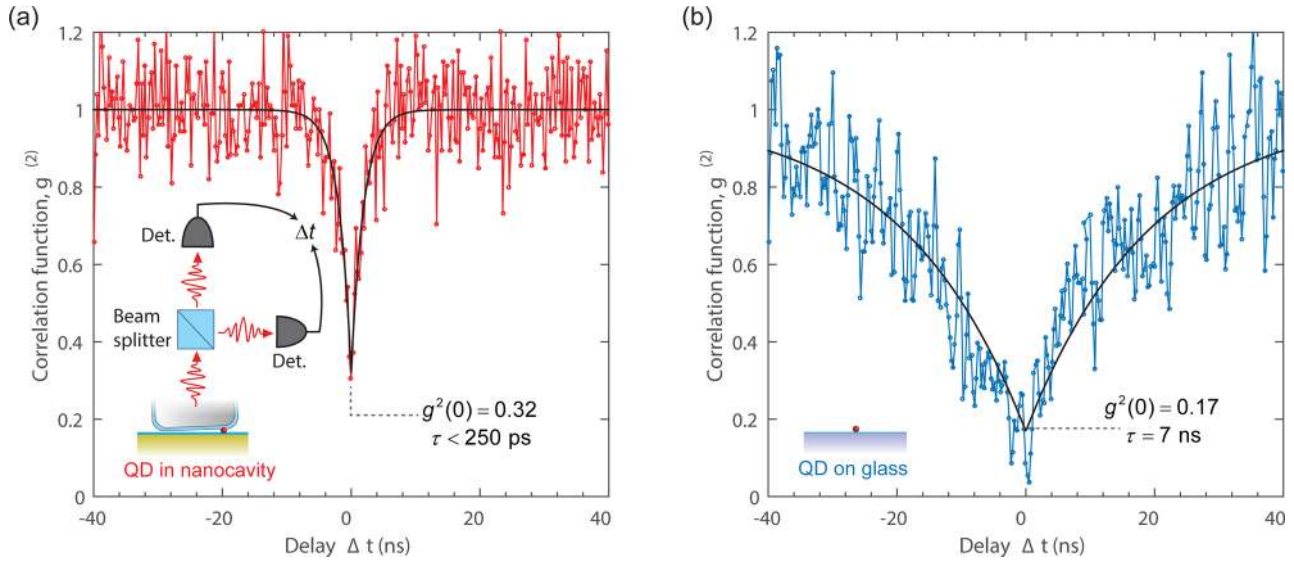

Figure 2. (a) Second-order photon correlation measurement, $g^2(t)$, from a nanocavity at an incident excitation power of 30 nW. The correlation function shows single antibunched photon emission with $g^2(0)$ = 0.32 and a decay lifetime of τ < 250 ps, which is limited by the 250 ps time bins used in this measurement. Inset shows diagram of the photon correlation measurement setup. (b) The correlation function for a single QD on glass, with $g^2(0)$= 0.17 and a much longer decay lifetime of τ = 7 ns. The $g^2(t)$ functions were normalized without subtracting the background due to the dark counts of the photodetectors (~20−30 counts/s).

spontaneous emission rate. At the same time, because of the optical antenna geometry, the emission is also highly directional and has a high quantum efficiency. The nanocavity is composed of a colloidally synthesized silver nanocube[27,28] separated from a gold film by a single colloidal QD and polymer layers (Figure 1a−c). Three nanometer polymer layers above and below the QD create a ~12 nm gap between the metal film and the nanocube, which supports a highly confined plasmonic cavity mode. The nanocavity can also be considered a nanoscale patch antenna that has a single radiation lobe normal to the surface, which has an angular full width of ~100°. Our previous work has demonstrated through simulations and Fourier-space imaging that the emission from these nanoantennas can be collected with 84% efficiency using a 0.9 NA objective.[23] Although these earlier measurements were done with ensembles of emitters, single optimally coupled emitters, such as QDs, couple to the same mode and hence should have the same radiation pattern in the far field.

The small mode volume cavity is defined by the bottom surface of the nanocube, the gold film, and the edges of the

DOI: 10.1021/acs.nanolett.5b03724
Nano Lett. XXXX, XXX, XXX−XXX

nanocube. The field confinement results in large enhancements in the spontaneous emission rate of dipole emitters embedded in the gap region. By using full-wave simulations, the Purcell enhancement is found to be spatially dependent across the nanocavity as shown in Figure 1, panel d. For randomly oriented dipoles, the largest enhancements occur near the corners of the nanocube and reach a factor of $F_p \approx 2000$, as determined from finite element simulations (Supporting Information). These large enhancements occur at the fundamental resonance of the nanocavity, which is identified by white light scattering spectra. Figure 1, panel e shows the white light scattering spectrum of a single antenna with a resonance wavelength of 630 nm for a nanocube dimension of ~75 nm. QDs are chosen with an emission spectrum at 630 nm to provide maximum spectral overlap with the plasmonic mode. Critically, the nanocavity also acts as an efficient optical antenna: emission that is coupled to the plasmonic mode is radiated into free space with high efficiency (~50%) and, as has been shown in prior work,[23] has a high collection efficiency using free space optics of ~84%. Additional loss mechanisms of the antenna, such as coupling to surface plasmon modes,[29] may contribute to a slightly lower radiative quantum efficiency.

The nanocavities are fabricated by spin coating CdSe/ZnS core−shell QDs on a 50 nm gold film coated with a 3 nm polymer adhesion layer (Methods section). The typical separation between QDs on the surface is greater than 100 nm, as determined by scanning electron microscopy (SEM) images of the sample (Figure 1c), to increase the probability of single QDs being coupled to the nanocavities. The silver nanocubes are deposited from solution and adhere to the polymer layer forming the nanocavities, some of which contain a single embedded QD. Nanocavities coupled to QDs are identified by photoluminescence (PL) imaging. Only nanocavities with a resonance wavelength of $\lambda \approx 630$ nm are selected, as determined from the white light scattering spectrum. Steady-state and time-resolved PL measurements were performed on the selected nanocavities using a diffraction limited laser spot. At present, the process of integrating single QDs into the nanocavities is statistical, determined by the random adhesion of nanocubes to regions that contain a single QD. We find that ~1% of nanocubes have an optimally coupled single QD in the gap region, as determined by fluorescence intensity measurements. Future work may exploit deterministic positioning of QDs in the nanocavities for optimal coupling, for example, using DNA-templated assembly.[30]

Figure 2, panel a shows the second order photon correlation measurement, $g^2(t)$, for a representative nanocavity coupled to a single QD, measured using a Hanbury−Brown Twiss setup with continuous-wave excitation at $\lambda = 488$ nm (Methods section). The correlation function shows a distinctive dip at $t = 0$ with $g^2(0) = 0.32$, which demonstrates the coupling of a single QD to the nanocavity. The residual correlated emission at $t = 0$ may be explained by detector dark counts, background fluorescence signal from nearby QDs, or weak multiphoton emission[31] from the coupled QD. However, if multiphoton emission is present, it is very weak because these measurements are performed well below the saturation intensity at which multiexciton generation and suppressed Auger recombination would occur and because the observed second order photon correlation measurement is well below 0.5 at $t = 0$. The decay lifetime of the correlation function has an upper bound of $\tau_{NPA} < 250$ ps, which is limited by the 250 ps time bin used in this measurement. Similar correlation results were obtained on ~12 other nanocavities each coupled to a single QD (Supplementary Figure 2). For comparison, a single QD on glass also shows single photon emission, with $g^2(0) = 0.17$, but with a much slower decay time of $\tau_{glass} = 7$ ns (Figure 2b). These measurements give a lower bound on the Purcell enhancement for a single QD of $F_p = 28$, which is limited by the time binning used in this measurement.

To better resolve the lifetime of the single photon emitter, we measured the time-resolved emission dynamics using pulsed excitation at $\lambda = 535$ nm and a single photon detector (Figure 3a). The same nanocavity as described in Figure 2 shows a biexponential decay with a fast lifetime of $\tau_{NPA} = 13$ ps from a fit to the data and is limited by the instrument response function (IRF) of the detector, which has a full-width at half-maximum of ~30 ps. The fitting was performed by convolving the measured IRF with a biexponential function. From the fit, it was determined that a large majority of the photons (97%) are emitted during the fast component of the decay. The slow component could be attributed to orthogonal emission dipoles of the QD[32] that are not optimally oriented relative to the dominant electric field component in the cavity. In contrast, a single QD on glass shows a PL decay lifetime of $\tau_{glass} = 6.8$ ns, in agreement with the lifetime obtained from the correlation

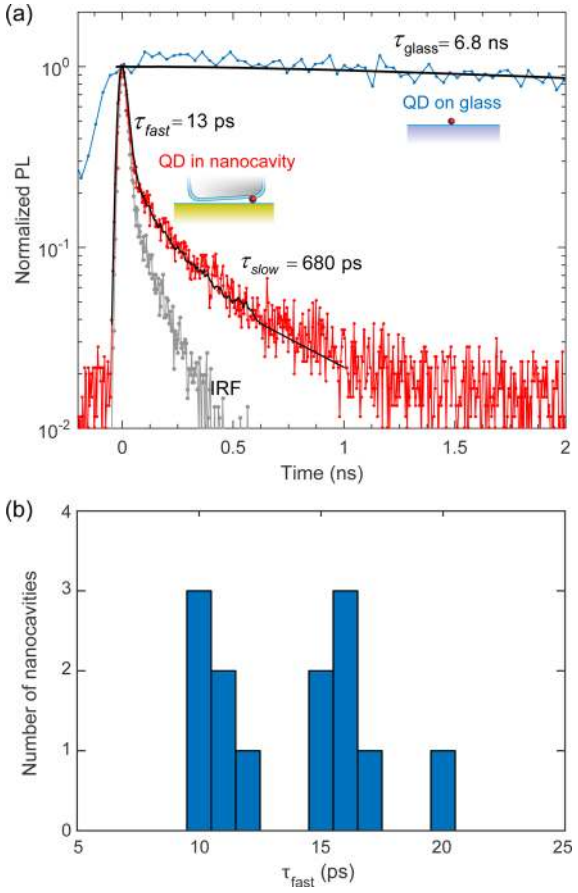

Figure 3. (a) Time-resolved PL from a single QD coupled to a nanocavity (red), showing a biexponential decay with a fast component of $\tau_{fast} = 13$ ps and a slow component of $\tau_{fast} = 680$ ps. The fast component is limited by the IRF of the avalanche photo diode detector, also shown (light gray). The lifetime of a single QD on glass is $\tau_{glass} = 6.8$ ns (blue). (b) Histogram of the extracted fast decay components of 13 coupled single QDs.

DOI: 10.1021/acs.nanolett.5b03724
Nano Lett. XXXX, XXX, XXX−XXX

measurements earlier (Figure 2b). QDs on a gold film without the nanocubes show weak emission with a relatively long lifetime of 0.8 ns,[25] indicating that excitation laser light or uncoupled QD emission are not contributing to the intense and fast emission seen in Figure 3. The observed decay lifetime of 13 ps indicates a detector-limited lower bound for the Purcell factor of $F_p \geq 540$ for a single QD coupled to a nanocavity. From the intrinsic quantum yield of QDs on glass of QY_0 = 20% and the quantum yield of the nanocavity of QY = 50%, the radiative rate enhancement for this single coupled quantum dot is $\gamma_r/\gamma_r^0 = (\tau_{glass}/\tau_{fast})(QY/QY_0) = 1350$. According to simulations, the Purcell factor (the enhancement in the total decay rate) approaches $F_p = 2000$ if the QD is optimally positioned near the corner. Similar decay dynamics were observed from 12 other coupled single QDs, and their extracted fast decay components are summarized in the histogram in Figure 3, panel b. Other nanocavities were observed that showed nonoptimal coupling to single QDs due to the random relative position between the nanocubes and the QDs.

A key question is whether the short emission lifetime is due to nonradiative plasmon decay or due to enhancement of the radiative rate. To answer this, we compare the time-averaged emission rate from a single QD on glass relative to a single QD coupled to the nanocavity described earlier, using continuous wave excitation at 488 nm (Figure 4). The coupled QD shows a

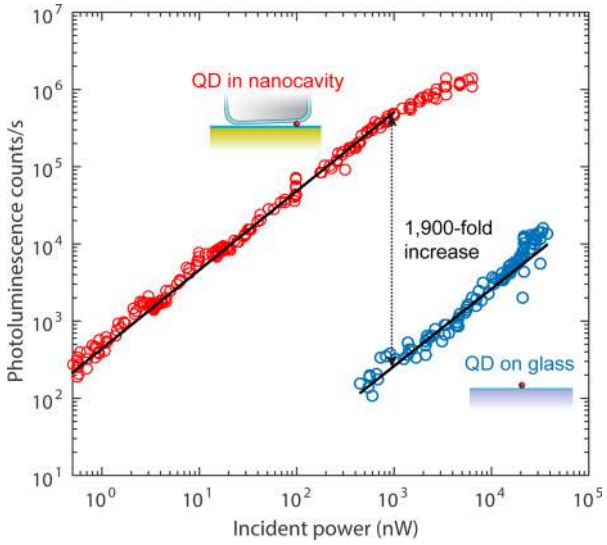

Figure 4. PL counts as a function of incident excitation power from a single QD coupled to a nanocavity (red) and a single QD on glass (blue). The PL intensity is linear with excitation power when the power is <1000 nW for the coupled case. The maximum detected count rate from this coupled QD in the linear regime is 1 MHz. Compared to the single QD on glass at the same excitation power, the emission intensity of the coupled QD is enhanced by a factor of 1900.

linear dependence between the excitation power and the emission rate for incident powers below 1 μW, with a detected count rate on the single photon detector of 500 kHz at 1 μW excitation. In comparison, a typical QD on glass shows a detected photon rate of 260 Hz at the same excitation power. This relatively low detected count rate from the QD control sample is due to the 1% transmission and detection efficiency of our setup, the use of a relatively low numerical aperture objective, and collection of fluorescence into free space rather than through the substrate into which most of the emission is coupled.

The 1900-fold increase in the steady-state emission rate from a single QD can be expressed by the fluorescence enhancement factor

$$EF = \frac{\eta}{\eta_0}\frac{\gamma_{ex}(\mathbf{r},\theta)}{\gamma_{ex}^0(\theta)}\frac{QY(\mathbf{r})}{QY_0}$$

which is composed of three factors. (1) The angular emission pattern of the QD is modified by the nanocavity such that the collection efficiency is estimated to be η = 84% using an objective lens with an NA = 0.9. Meanwhile, a randomly oriented QD on glass has a collection efficiency of only η_0 = 19% using the same objective. (2) The QD absorption rate at position $\mathbf{r}$ and dipole orientation angle θ in the nanocavity is γ_{ex}, which is enhanced relative to the excitation rate in free space, γ_{ex}^0, even under nonresonant excitation at 488 nm. The enhancement in the excitation rate is calculated to be a factor of $\gamma_{ex}/\gamma_{ex}^0 = 225$ for a vertically oriented dipole near the corner of the nanocube where the largest Purcell factors occur (Supplementary Figure 1). (3) The radiative quantum yield of the emitter is modified by the nanocavity and is predicted to be QY = 50% relative to the estimated quantum yield of QY_0 = 20% for QDs on glass. This intrinsic quantum yield is inferred from the 7 ns measured PL lifetime of QDs on glass and the 32 ns radiative lifetime for CdSe core−shell QDs in solution.[33] By combining all three effects, we predict a total emission enhancement of EF = 2500, which is in qualitative agreement with the maximum measured enhancement of EF = 1900. This agreement indicates that the quantum yield for emission of photons is high for optimally coupled QDs and that the large Purcell factor is due to an enhanced radiative rate rather than nonradiative quenching. Additionally, by comparing the count rates from single QDs coupled to eight nanocavities and 12 single QDs on a glass slide, we extracted an average enhancement factor of EF = 495, indicating situations in which the QDs are not optimally situated under the nanocubes.

Having established the ultrafast decay dynamics due to Purcell enhancement and high quantum efficiency, we now discuss the achievable count rates and future prospects for this plasmonic platform. Given the maximum detected count rate of 1 MHz and the calculated 1% transmission and detection efficiency of the setup, we estimate that the collected photon count rate into the objective lens is 100 MHz. Saturation of the QD emission was not possible due to eventual photobleaching. Given the short (<13 ps) excited state lifetime of the QD, saturation is expected to occur at an emission rate of ~80 GHz. In the future, these count rates could be achieved by integrating more photostable emitters into the nanocavity such as color centers in diamond[34] or silicon carbide.[11]

The plasmonic nanocavity coupled to a single QD acts as a single photon source operating in the regime of ultrafast spontaneous emission at room temperature. The detector limited emission lifetime of 13 ps corresponds to a 540-fold enhancement in the spontaneous emission rate of the QD and points toward a single photon source operating at a rate exceeding 80 GHz. The maximum ~1900-fold enhancement in the time-averaged emission intensity from the single QD shows that the fast emission lifetime is due to enhancement of the radiative rate rather than quenching. Furthermore, the antenna action of the cavity results in a directional radiation pattern and allows for high collection efficiency by free space optics or into

DOI: 10.1021/acs.nanolett.5b03724
Nano Lett. XXXX, XXX, XXX−XXX

a single mode fiber. By utilizing techniques developed for dielectric cavities,[16] single emitters could be deterministically positioned and oriented, resulting in even larger enhancements. Additionally, electrical excitation in this structure is promising for future high-speed on-demand single photon generation.

Methods. *Sample Preparation.* The nanocavities are fabricated by first depositing a gold film onto a clean glass substrate by electron beam evaporation (5 nm Ti, 50 nm Au). The sample was immersed in a 3 mM solution of poly(allylamine hydrochloride) (PAH) for 5 min, 3 mM polystyrenesulfonate (PSS) for 5 min, and terminated with a final step in PAH for 5 min. After each step (PAH or PSS), the sample was rinsed with ultrapure deionized water and 1 min in 1 M NaCl. Each PAH/PSS step deposits a ∼1 nm polymeric film with a surface positive/negative charge, and a final PAH layer is used to promote adhesion of the negatively charged QDs and nanocubes. CdSe/ZnS core−shell QDs (Sigma-Aldrich) with a peak emission wavelength of 630 nm and oleic acid ligands were diluted to a concentration of 0.01 mg/mL in toluene. The diluted solution was spin coated onto the prepared gold/PAH substrates at a speed of 1500 rpm for 60 s.

Silver nanocubes were synthesized by reduction of $AgC_2F_3O_2$ using a previously described method.[35] Following synthesis, the nanocubes were centrifuged at 1500 rpm to select silver particles of the desired size (∼75 nm) and resuspended in deionized water. The stock nanocube solution was diluted 100-fold; a droplet of the diluted solution was deposited on the sample and then covered with a glass slide. This step allows the nanocubes to adhere to the PAH layer. After 5 min, the nanocube solution was washed off with water and the sample dried with nitrogen gas.

Optical Measurements. Nanocavities were investigated on a custom-built microscope,[23] with all measurements done at room temperature. A laser beam (continuous wave 488 nm wavelength, 1 mW power) was defocused and sent onto the sample through a 100× , NA = 0.9 objective. The PL was collected through the same objective and passed through a 600 nm long-pass fluorescence filter and imaged onto an electron multiplying charged coupled device camera. Nanocavities resonant with one or more QDs appeared as bright diffraction limited spots in the PL image. These identified particles were moved to the center of the field of view and illuminated with white light through a dark field objective. Scattered light from a single nanocavity was imaged onto an imaging spectrograph to determine the plasmon resonance. Only nanocavities with a resonance of ∼630 nm were selected to ensure good spectral overlap with QD emission. Once selected, the nanocavity is excited with a focused continuous wave laser (488 nm wavelength) at an incident power of <100 nW. To verify the presence of a single QD, the PL is split by a nonpolarizing beamsplitter and imaged onto a pair of single-photon counting avalanche photodiodes (APD, 50 μm^2 active area, Micro Photon Devices). The detectors are connected to a time-correlated single photon counting module (Picoharp 300, PicoQuant Inc.) that measures the arrival times between photons on the two detectors, producing the second order correlation function. To measure the decay lifetimes in Figure 3, a pulsed laser (535 nm wavelength, 80 MHz repetition rate, 30 nW power) is used to excite the nanocavity, and the PL is imaged onto a single APD with the arrival time of the photons recorded relative to the laser pulse arrival.

■ ASSOCIATED CONTENT

Supporting Information

The Supporting Information is available free of charge on the ACS Publications website at DOI: 10.1021/acs.nanolett.5b03724.

Simulations of excitation field enhancement and time-resolved emission data for additional nanocavities (PDF)

■ AUTHOR INFORMATION

Corresponding Author

*E-mail: m.mikkelsen@duke.edu.

Author Contributions

T.B.H. and G.M.A. contributed equally to this work. M.H.M. conceived and designed the experiments. T.B.H. synthesized the nanocubes, fabricated the samples, and performed the experiments. G.M.A. built the experimental setup. T.B.H. and G.M.A. analyzed the data. G.M.A. and M.H.M. wrote the manuscript. M.H.M. supervised the project.

Notes

The authors declare no competing financial interest.

■ ACKNOWLEDGMENTS

This work was supported by a Faculty Early Career Development Program (CAREER) award from the National Science Foundation (DMR-1454523). G.M.A. acknowledges support from the Intelligence Community Postdoctoral Research Fellowship Program.

■ REFERENCES

(1) Eisaman, M. D.; Fan, J.; Migdall, A.; Polyakov, S. V. *Rev. Sci. Instrum.* **2011**, *82*, 071101.
(2) Shields, A. J. *Nat. Photonics* **2007**, *1*, 215−223.
(3) Lee, K. G.; Chen, X. W.; Eghlidi, H.; Kukura, P.; Lettow, R.; Renn, A.; Sandoghdar, V.; Gotzinger, S. *Nat. Photonics* **2011**, *5*, 166−169.
(4) Vittorio, M. De; Pisanello, F.; Martiradonna, A.; Qualtieri, A.; Stomeo, T.; Bramati, A.; Cingolani, R. *Opto-Electronics Rev.* **2010**, *18*, 1−9.
(5) Naiki, H.; Masuo, S.; Machida, S.; Itaya, A. *J. Phys. Chem. C* **2011**, *115*, 23299−23304.
(6) Claudon, J.; Bleuse, J.; Malik, N.; Bazin, M.; Jaffrennou, P.; Gregersen, N.; Sauvan, C.; Lalanne, P.; Gerard, J. *Nat. Photonics* **2010**, *4*, 174−177.
(7) Holmes, M. J.; Choi, K.; Kako, S.; Arita, M.; Arakawa, Y. *Nano Lett.* **2014**, *14*, 982−986.
(8) Schietinger, S.; Barth, M.; Aichele, T.; Benson, O. *Nano Lett.* **2009**, *9*, 1694−1698.
(9) Choy, J.; Hausmann, B.; Babinec, T.; Bulu, I.; Khan, M.; Maletinsky, P.; Yacoby, A.; Loncar, M. *Nat. Photonics* **2011**, *5*, 738−743.
(10) Faraon, A.; Barclay, P. E.; Santori, C.; Fu, K.-M. C.; Beausoleil, R. G. *Nat. Photonics* **2011**, *5*, 301−305.
(11) Castelletto, S.; Johnson, B.; Ivády, V.; Stavrias, N.; Umeda, T.; Gali, A.; Ohshima, T. *Nat. Mater.* **2013**, *13*, 151−156.
(12) Purcell, E. *Phys. Rev.* **1946**, *69*, 681.
(13) Albrecht, R.; Bommer, A.; Deutsch, C.; Reichel, J.; Becher, C. *Phys. Rev. Lett.* **2013**, *110*, 243602.
(14) Englund, D.; Fattal, D.; Waks, E.; Solomon, G.; Zhang, B.; Nakaoka, T.; Arakawa, Y.; Yamamoto, Y.; Vučković, J. *Phys. Rev. Lett.* **2005**, *95*, 013904.
(15) Vučković, J.; Fattal, D.; Santori, C.; Solomon, G. S.; Yamamoto, Y. *Appl. Phys. Lett.* **2003**, *82*, 3596−3598.
(16) Hennessy, K.; Badolato, A.; Winger, M.; Gerace, D.; Atatüre, M.; Gulde, S.; Fält, S.; Hu, E. L.; Imamoğlu, A. *Nature* **2007**, *445*, 896−899.

DOI: 10.1021/acs.nanolett.5b03724
Nano Lett. XXXX, XXX, XXX−XXX

(17) Kinkhabwala, A.; Yu, Z.; Fan, S.; Avlasevich, Y.; Mullen, K.; Moerner, W. *Nat. Photonics* **2009**, *3*, 654−657.
(18) Gong, S.-H.; Kim, J.-H.; Ko, Y.-H.; Rodriguez, C.; Shin, J.; Lee, Y.-H.; Dang, L. S.; Zhang, X.; Cho, Y.-H. *Proc. Natl. Acad. Sci. U. S. A.* **2015**, *112*, 5280−5285.
(19) Curto, A. G.; Volpe, G.; Taminiau, T. H.; Kreuzer, M. P.; Quidant, R.; van Hulst, N. F. *Science* **2010**, *329*, 930−933.
(20) Ratchford, D.; Shafiei, F.; Kim, S.; Gray, S. K.; Li, X. *Nano Lett.* **2011**, *11*, 1049−1054.
(21) Kolchin, P.; Pholchai, N.; Mikkelsen, M. H.; Oh, J.; Ota, S.; Islam, M. S.; Yin, X.; Zhang, X. *Nano Lett.* **2015**, *15*, 464−468.
(22) Esteban, R.; Teperik, T. V.; Greffet, J. J. *Phys. Rev. Lett.* **2010**, *104*, 026802.
(23) Akselrod, G. M.; Argyropoulos, C.; Hoang, T. B.; Ciracì, C.; Fang, C.; Huang, J.; Smith, D. R.; Mikkelsen, M. H. *Nat. Photonics* **2014**, *8*, 835−840.
(24) Belacel, C.; Habert, B.; Bigourdan, F.; Marquier, F.; Hugonin, J.-P.; de Vasconcellos, S. M.; Lafosse, X.; Coolen, L.; Schwob, C.; Javaux, C.; Dubertret, B.; Greffet, J.-J.; Senellart, P.; Maitre, A. *Nano Lett.* **2013**, *13*, 1516−1521.
(25) Hoang, T. B.; Akselrod, G. M.; Argyropoulos, C.; Huang, J.; Smith, D. R.; Mikkelsen, M. H. *Nat. Commun.* **2015**, *6*, 7788.
(26) Yuan, C. T.; Wang, Y. C.; Cheng, H. W.; Wang, H. S.; Kuo, M. Y.; Shih, M. H.; Tang, J. *J. Phys. Chem. C* **2013**, *117*, 12762−12768.
(27) Sun, Y.; Xia, Y. *Science* **2002**, *298*, 2176−2179.
(28) Rycenga, M.; Xia, X.; Moran, C. H.; Zhou, F.; Qin, D.; Li, Z.-Y.; Xia, Y. *Angew. Chem., Int. Ed.* **2011**, *50*, 5473−5477.
(29) Pors, A.; Bozhevolnyi, S. I. *ACS Photonics* **2015**, *2*, 228−236.
(30) Lin, Q.-Y.; Li, Z.; Brown, K. a.; O'Brien, M. N.; Ross, M. B.; Zhou, Y.; Butun, S.; Chen, P.-C.; Schatz, G. C.; Dravid, V. P.; Aydin, K.; Mirkin, C. A. *Nano Lett.* **2015**, *15*, 4699−4703.
(31) Nair, G.; Zhao, J.; Bawendi, M. *Nano Lett.* **2011**, *11*, 1136−1140.
(32) Bawendi, M.; Empedocles, S.; Neuhauser, R. *Nature* **1999**, *399*, 126−130.
(33) Chen, O.; Zhao, J.; Chauhan, V. P.; Cui, J.; Wong, C.; Harris, D. K.; Wei, H.; Han, H.-S.; Fukumura, D.; Jain, R. K.; Bawendi, M. G. *Nat. Mater.* **2013**, *12*, 445−451.
(34) Bradac, C.; Gaebel, T.; Naidoo, N.; Sellars, M. J.; Twamley, J.; Brown, L. J.; Barnard, a S.; Plakhotnik, T.; Zvyagin, a V; Rabeau, J. R. *Nat. Nanotechnol.* **2010**, *5*, 345−349.
(35) Zhang, Q.; Li, W.; Wen, L.-P.; Chen, J.; Xia, Y. *Chem. - Eur. J.* **2010**, *16*, 10234−10239.

DOI: 10.1021/acs.nanolett.5b03724
Nano Lett. XXXX, XXX, XXX−XXX